Gröschl, Jasmin Katrin; Steinwachs, Thomas

Working Paper

Borders, Roads and the Relocation of Economic Activity Due to Extreme Weather

CESifo Working Paper, No. 8193

Provided in Cooperation with:
Ifo Institute – Leibniz Institute for Economic Research at the University of Munich

Suggested Citation: Gröschl, Jasmin Katrin; Steinwachs, Thomas (2020) : Borders, Roads and the Relocation of Economic Activity Due to Extreme Weather, CESifo Working Paper, No. 8193, Center for Economic Studies and ifo Institute (CESifo), Munich

This Version is available at:
https://hdl.handle.net/10419/216589

CESifo WORKING PAPERS

8193
2020

March 2020

Borders, Roads and the Relocation of Economic Activity Due to Extreme Weather

Jasmin Gröschl, Thomas Steinwachs

CESifo

Impressum:

CESifo Working Papers
ISSN 2364-1428 (electronic version)
Publisher and distributor: Munich Society for the Promotion of Economic Research - CESifo GmbH
The international platform of Ludwigs-Maximilians University's Center for Economic Studies and the ifo Institute
Poschingerstr. 5, 81679 Munich, Germany
Telephone +49 (0)89 2180-2740, Telefax +49 (0)89 2180-17845, email office@cesifo.de
Editor: Clemens Fuest
https://www.cesifo.org/en/wp
An electronic version of the paper may be downloaded
· from the SSRN website: www.SSRN.com
· from the RePEc website: www.RePEc.org
· from the CESifo website: https://www.cesifo.org/en/wp

CESifo *Working Paper No. 8193*

Borders, Roads and the Relocation of Economic Activity Due to Extreme Weather

Abstract

Extreme weather may give rise to the relocation of economic activity towards nearby locations. But how are the economic effects of weather events transmitted between locations? And, which role does the interconnection of small economic units play? This paper takes a granular approach to identify the role of connectivity on economic activity due to severe weather. We combine a 0.5°×0.5° grid-cell level dataset on economic activity and weather events with global geographic information on national borders and road networks. We first explore how a potential disruption of connectivity through an international border affects local spillovers in case of a weather shock. Second, we use road infrastructure as a proxy for overall connectivity to explore how this affects the diversion of economic activity across local economic units. Results suggest that international borders limit economic relocation due to extreme weather to domestic neighboring cells. The existence of major road infrastructure between locations is key to the relocation of economic activity due to a weather event. Without a transport network, spillovers between local economic units do, on average, not exist or are at least very limited and costly to implement.

JEL-Codes: F150, O180, Q540, R110.

Keywords: light emission, weather, connectivity, border effect, road network.

Jasmin Gröschl
ifo Institute – Leibniz Institute for Economic Research at the University of Munich
Germany – 81679 Munich
groeschl@ifo.de

Thomas Steinwachs
ifo Institute – Leibniz Institute for Economic Research at the University of Munich
Germany – 81679 Munich
thomas.steinwachs@gmail.com

March 23, 2020

The authors thank Vincent Stamer for able research assistance and Andrew Bernard, Gabriel Felbermayr, Ilan Noy, Yoto Yotov and participants of the 2018 Annual Congress of the German Economic Association (Verein für Socialpolitik) for valuable comments and suggestions. The authors gratefully acknowledge the compute and data resources provided by the Leibniz Supercomputing Centre (www.lrz.de). Jasmin Gröschl gratefully acknowledges funding from the German Science Foundation (DFG) under project GR4896/1-1. Thomas Steinwachs acknowledges funding from the Leibniz Association under project SAW-2016-PIK-1. All remaining errors belong to the authors.

1. Introduction

The economic consequences of global warming have found soaring attention in recent years. A growing literature surveyed by Cavallo and Noy (2011) investigates the effect of natural disasters on economic growth. As extreme weather may have economic consequences, it is important to understand potential transmission channels and think about mitigation and adaptation mechanisms (cf. Fisher et al., 2012; Deschênes and Greenstone, 2012; Burke and Emerick, 2016). But how are the economic effects of weather events transmitted between locations? And, which role does the interconnection of small economic units play? While connectivity within and between countries matters for economic growth due to more efficient and productive markets (World Bank, 2019), connectivity to international markets and border efficiency greatly increase the prospects of cooperation between countries and facilitate trade and economic growth (Buchan et al., 2012).

In this paper, we ask how the economic effects of severe weather transmit between locations. On a granular level, we examine how the spillover of economic activity is affected by international borders and by available road infrastructure. As country boundaries constitute frictions to the diversion of goods, information, financial flows, and people, we explore how national borders limit local spillovers due to a weather event. As the level of connectivity of a struck location is likely to be a driver of observed transactions, we use road infrastructure as a proxy for overall connectivity to explore how this promotes the relocation of economic activity across small economic units with extreme weather.

Previous studies either use cross-country data (e.g., Felbermayr and Gröschl, 2014) or focus on very specific regions and episodes (e.g., Strobl, 2011). But weather shocks are often local events and affect small countries differently than large ones (Noy, 2009). Mapping them to countries of heterogeneous size may result in measurement error and attenuation bias.[1] Felbermayr et al. (2018) take a granular approach to study the economic effects of natural disasters on light emissions, a proxy for local economic activity (cf. Storeygard, 2016; Henderson et al., 2012, 2017). Their analysis of 24,000 geographical units in 197 countries over 21 years suggest strong evidence for negative local disaster and transaction effects that phase out quickly over distance.[2] But the mechanisms through which disaster effects propagate across space remain in the dark.

On the country level, Felbermayr and Gröschl (2014) show that trade or financial openness and institutions facilitate mitigation in the case of disasters. Using a quantitative

[1] Strobl (2011) shows for the U.S. that hurricane effects are netted out at the state level and no effects are found on national economic growth rates.

[2] If neighboring areas specialize in the same production as directly affected cells, economic activity shifts, increasing the (value of) output in adjacent regions (cf. Hsieh and Ossa, 2016).

model with high-resolution data on agricultural productivity, Costinot et al. (2016) point out that international trade attenuates the costs of climate change, but only weakly. Like-minded, Desmet and Rossi-Hansberg (2015) analyze the impact of climate change on the spatial distribution of economic activity, trade, migration and welfare. They show that adaptation policies interact with innovation and the spatial pattern of economic activity. In this context, local geographic connectivity plays a major role in transmitting the effects from extreme weather. Closely connected locations should find it easier to respond to weather events by importing more from other areas or by allowing people to escape the consequences by relocating to less affected nearby places. However, national borders have been shown to constitute barriers to economic transactions (cf. Anderson and Van Wincoop, 2004; Chen, 2004). Contrary, road networks provide a potential mediating factor (cf. Banerjee et al., 2012; Faber, 2014). In a study based on night-time light emissions, Storeygard (2016) examines how road networks in Africa affect subnational economic growth due to oil price shocks. Similarly, Amarasinghe et al. (2018) use a network model to examine how spillovers from changes in mineral prices propagate through African road networks. Hence, we focus on the role of international borders and road networks for the transmission of economic effects in response to weather events.

Our findings support that severe weather generally hampers the growth of local economic activity. We find that the connectivity of cells is a main driver of economic relocation caused by weather events. For national borders, results suggest increased localization and a fragmentation of production across countries. Domestic cells are, on average, the exclusive sources of diversion for wind and precipitation events. For cold waves, domestic relocation shows 1.5 times significantly stronger effects than foreign cells. Next, we explore the impact of the existence of road infrastructure, as connectivity along major transport routes potentially eases travel time and reduces transport costs. Results indicate that the availability of at least one major road exclusively drives the diversion of economic activity for precipitation events. For cold waves, economic relocation effects are 3.5 times as strong for connected compared to unconnected neighboring cells. Finally, we examine whether the number of available road connections matters. For precipitation and cold events, estimates show stronger spillover effects for neighbors with a connectivity index above the local median connectedness. This confirms that relocation across highly connected neighbors is stronger than transactions across worse and thus more costly connections. Overall, our results suggest that international borders contain economic relocation activity due to weather events within the local domestic neighborhood. Then again, the

existence of major road infrastructure between locations is key to economic relocation of goods or people due to severe weather.

The remainder of the paper is organized as follows: Section 2 describes the data and the connectivity measures. Section 3 presents the empirical strategy. Section 4 provides results, followed by robustness checks in Section 5. The final section concludes.

2. Data

This paper combines two data sources: First, we use the Gridded GAME Database on weather events, including yearly information on global night-light emissions and population, as introduced by Felbermayr et al. (2018). Second, to analyze the transmission of spillover effects triggered by severe weather, we match this information with data on national borders and major roads. We describe in detail how we extract a grid-cell level indicator on border and road connectivity and discuss the properties.

2.1. Weather Events and Economic Activity

The Gridded GAME Database on geological and meteorological events, described in detail by Felbermayr et al. (2018), partitions the globe into small economic units along latitude and longitude, an approach also advocated by Nordhaus and Chen (2009) and Costinot et al. (2016). The balanced panel comprises 24,184 grid cells with a resolution of 0.5°×0.5° (approximately 55×55 km at the equator) spread across 197 countries from 1992 to 2013. Along with economic variables, it provides physical intensities of exogenous events, such as wind speeds, extreme precipitation, or cold waves. Wind speeds combine the maximum wind from a hurricane wind field model and interpolated information from weather stations. Extreme precipitation is identified through remotely-sensed precipitation anomalies above the local monthly long-run average. Cold waves use satellite data on temperature anomalies below the local monthly long-run average. To align with the temporal resolution of the dependent variable, all monthly weather indicators are aggregated to the yearly level by computing time-weighted averages over a rolling window (cf. Felbermayr et al., 2018).[3]

Economic activity, the dependent variable, is proxied by remotely-sensed data on global night-light emissions. The data come as yearly composite satellite images from the US Air Force Defense Meteorological Satellite Program (DMSP). From this, yearly mean light

[3]This allows each event to affect light emissions for exactly 12 months. The rolling window is calculated by $\frac{1}{n}\sum_{t=0}^{n-1} p_{month-t}$.

emissions are extracted as a digital number (DN). To prepare the data for econometric analysis, we follow Felbermayr et al. (2018). In a nutshell, we crop all off-shore light pixels, mask misleading light sources like gas-flaring zones (Elvidge et al., 2009) and active volcanoes, select satellite sources by coverage quality for years in which multiple satellites are available, and mask pixels from the data for which the number of valid nights is zero. Finally, we aggregate night-light pixels to mean light intensity at the $0.5°\times0.5°$ grid cell level. Night-light emission data has widely been used as a proxy for economic activity in empirical analysis. Henderson et al. (2012) and Storeygard (2016) find a lights-to-GDP growth elasticity of around 0.3 at the country and the Chinese prefecture level, respectively. Felbermayr et al. (2018) find strong similarity between the elasticities of lights-to-population density and of GDP-to-population density, fostering the adequacy of night-light emissions as a proxy for economic activity.

Grid cell level population is used as a control variable. Information on five-year target estimates at pixel level stem from the Gridded Population of the World (GPW) project.[4] To obtain grid cell population numbers, we sum all pixel values within each cell and fill the gaps between given five-year periods by exponential interpolation. This assumes no excessive fluctuations in population within the five-year windows.

2.2. Border Connectivity

To measure whether neighboring economic units belong to the same country, we map cells to countries along 2011 global country boundaries. National borders are defined in the high resolution Biogeo World Map Shape File provided by the University of California, Davis.[5] A grid cell coincides with at most four countries. As our empirical strategy requires an unambiguous mapping between cells and countries, we select the main country based on the relative size of its land area within a cell, if necessary.

2.3. Road Infrastructure Connectivity

To measure globally consistent road infrastructure connectivity, we feed remote-sensing information on global road networks into a modified Dijkstra (1959) search algorithm. The Dijkstra algorithm solves the problem of finding the shortest route between a start node and a destination node via an arbitrary number of intermediate nodes connected by paths on a predefined network. Each path holds a non-negative cost weight. In our case,

[4]The data are based on census inputs collected at the lowest administrative units available, which are redistributed from their administrative census boundaries to a uniform grid by using aerial weights.

[5]https://biogeo.ucdavis.edu/projects.html

nodes represent grid cells within a local neighborhood defined by a constant metric search radius r. The cell in the center of the neighborhood defines the start node, whereas all its neighbors serve as either intermediate or destination nodes. Paths represent distances between all pairs of adjacent nodes connected by roads.

Geographic information on road networks stem from the Environmental Systems Research Institute (Esri, 2016), who provide a globally consistent shape file of important road connections according to the DeLorme World Base Map.[6] It provides a global road network snapshot based on satellite images collected between 1999 and 2008.[7] The data include 73,325 highways, 78,911 major roads, 3,373 local roads and 399 ferry connections.[8] Direct routing is not feasible globally as separate road shapes are not always continuously connected. Moreover, non-observed smaller road connections between observed major roads may exist. We address both issues by calculating the number of distinct roads leading from one cell to an adjacent cell in terms of intersections between road shapes and cell-border polygons. Each intersection adds one path to the network. Each path is associated with a distance proxy, our cost weight. This proxy reflects the overall distance between cells and accounts for intra-cell travel distance.

As a result of global curvature, distances vary across cells due to varying metric correspondence to one degree longitude lon across latitude lat, and because coastal cells are typically associated with smaller land area a. Hence, we define the distance weight of a cell by the latitudinal mean and the ratio between this dimension and the land area. To approximate travel distance between adjacent cells, we take the average of individual distance weights. Bilateral distance d^c for two adjacent cells is

$$d^c = \frac{1}{4} \sum_{i=1}^{2} \left(\frac{a^i \text{ km}^2}{lat^i \text{ km}} + lat^i \text{ km} \right). \tag{1}$$

The search algorithm constructs the shortest-path tree from the start node via all viable routes within the neighborhood for each local destination. Each iteration picks the unvisited node within the shortest distance d^c and computes the distance through this node to each unvisited adjacent cell. If the distance along this path is smaller than any distance found in a previous iteration (or the starting value), the information is updated.

[6]This map is compiled by Garmin International, Inc. from satellite imagery captured by Landsat 7 (Global Land Surveys 2000 and 2005) and the Shuttle Radar Topography Mission (SRTM).

[7]Global consistency is a key prerequisite for our approach. Many available road shape files (e.g., Open Street Map) are more detailed but have either strong coverage biases for certain world regions or are not cleaned, such that non-reasonable road patterns emerge in some locations.

[8]Ferries constitute an important source of connectivity, especially for islands and will be treated as roads henceforth.

The algorithm stops once the shortest path from the start cell to destination has been found. The distance from the centroid cell to destination is thus the sum of bilateral cell distances over all nodes that jointly define the shortest path, $d = \sum_c d^c$.

The connection by multiple roads potentially increases the ease of transportation and communication between cells and allows for diversion if a road is congested or temporarily non-accessible. Next, we thus construct a measure that reflects the number of roads. We allow two adjacent cells to be connected by multiple paths, where each path can only be part of one route for any pair of cells. The connectivity measure is then calculated as a mean over the distances d_k along the k shortest routes. If we identify less than k viable routes for a connection between a given start and destination pair, we put a constant penalty distance p for each missing route. [9] The resulting indicator is

$$C = (1 - \bar{d}/p) \ , \tag{2}$$

where $\bar{d} = \frac{1}{k} \sum_{k=1}^{k} d_k$ is the mean distance along the k shortest routes and $1/p$ is the inverse penalty for missing connections (a scaling factor). Consequently, C is constrained to the $[0, 1[$ interval.[10] For the baseline specification, we consider the availability of up to three separate routes, $k = 3$.[11] Finally, note that by confining nodes to cells within a given search radius, we introduce asymmetries into the connectivity matrix whenever a potential node that could lead to a shorter path between A and B is located just outside the search radius around A but within the search radius around B. Since the econometric strategy requires symmetric weights matrices, asymmetric dyads are resolved by using the mean of the two deviating connectivity values.

2.4. Descriptives

Next, we examine the properties of the connectivity measure. Figure 1 shows the distribution of the mean connectivity of each cell within an 80 km radius for the balanced sample. It indicates substantial heterogeneity across and within countries. Local connec-

[9] The penalty equals the local neighborhood radius r plus half the neighborhood's circumference ($p = r + \pi r$). This represents the longest plausible geometric distance between the centroid and a point 180° into the opposite direction. Technically, p also serves as the starting value of each routing iteration.

[10] By definition, a connectivity of 1 applies only to the connectivity of each cell with itself, where distance is zero. Note that disentangling local spillover effects requires that a cell by itself must be excluded from its own set of neighbors. A value of 0 indicates $\bar{d} = p$, the longest possible mean distance.

[11] A smaller k implies that more weight is given to the shortest route. A higher k increases the right-skew of the connectivity distribution as it raises the likelihood of penalties (see Section 2.4 for details). For robustness, we consider $k = 1$ as an alternative case.

tivity appears higher in industrialized countries, is clustered around economic centers and shows a natural decay around mountainous, desertified terrain, and islands.

Figure 1: Global Connectivity Distribution

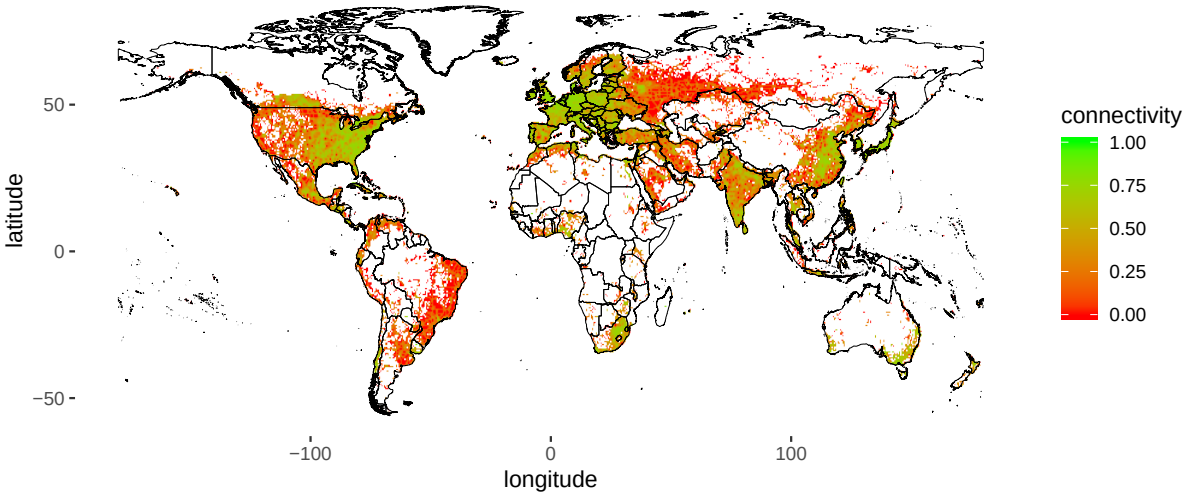

Note: Sources: Biogeo World Map Shape File (UC Davis), own calculations. Time-constant mean connectivity index realizations of locations within a local neighborhood (80 km radius) for the balanced panel. Higher index values imply higher connectivity.

Figure 2a depicts the cross-sectional correlation between cell connectivity and light emission in 2013. It suggests that light emission tends to cluster in locations that are well-connected with their local neighbors by road. Note, it also shows that a significant number of cells (one fifth of the sample) are not connected by important roads but still exhibit substantial night light.[12] Figure 2b compares the distribution of light emission of unconnected cells (i.e., zero connectivity in Figure 2a) with those that are connected with at least one neighbor. While both distributions follow a bell-shape, connected cells have stronger absolute night-light emission than unconnected cells. Figure 2c shows the kernel densities of mean connectivity by continent. South America and Asia have the highest frequency of disconnected cells and the lowest proportion of highly-connected cells. Interestingly, the proportion of disconnected cells in Africa is lower than in South America, Asia and North America. This implies that, once a location in Africa is sufficiently active to be reflected in the night-light data, it has a relatively good road connectivity within its neighborhood. The density function for North America has two local maxima, representing the divide between highly connected locations in the East and lowly to intermediately connected cells in the West. Finally, Europe's left-skewed density function supports the

[12]Figure A1 in the Appendix depicts roads connectivity versus light growth. The flat line indicates that endogeneity is not an issue in the connectivity light context.

very advanced infrastructure and interconnectedness of the continent. The heterogeneity in the connectivity distribution across continents suggests that identification should focus on local rather than global statistics to capture the (relative) connectivity of locations within their neighborhood rather than systematic differences across the globe.

Figure 2: Connectivity Descriptives

(a) Connectivity vs. Activity

(b) Connected vs. Unconnected

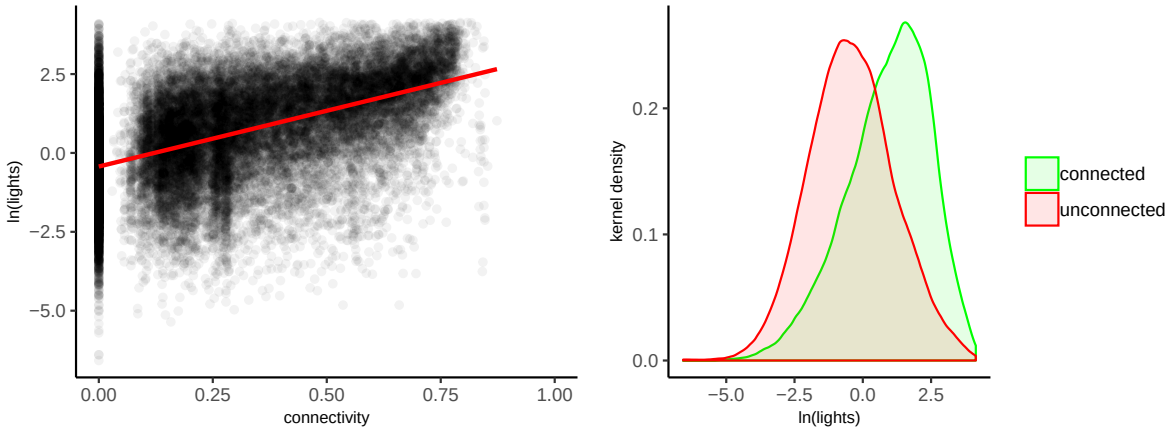

(c) Connectivity by Continents

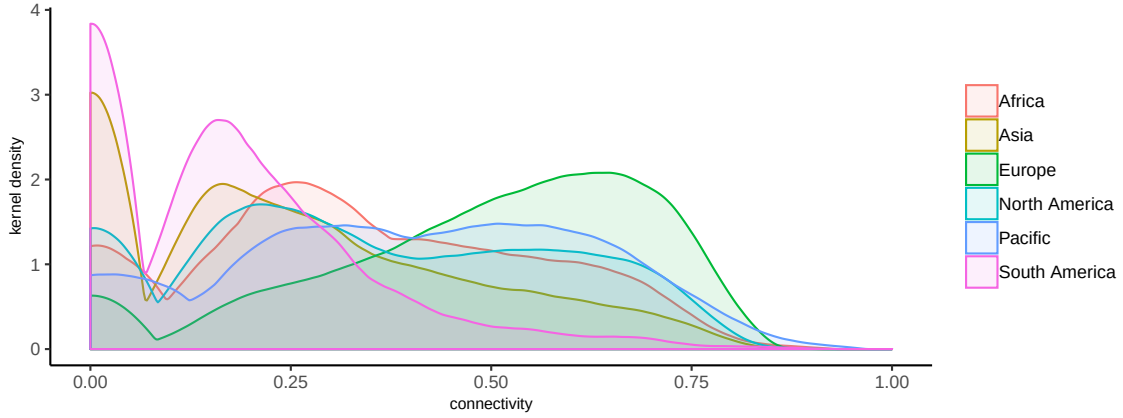

Note: Plotted ln(lights) represent absolute logarithmic values in 2013. Epanechnikov Kernel used to compute densities.

Figure 3 zooms in on selected locations to visualize the bilateral connectivity of each surrounding cell with the respective centroid. In the case of Sydney, Australia the highest connectivity exists with the cell to the West, to which the city extends to a large part, and to the South, which contains an economically active land area in its upper left corner closely connected to the city. The cell to the South-West of Sydney contains the fairly connected suburban areas around Campbelltown. Connectivity is lower to the North. These cells mainly cover buildup areas in and beyond the Marramarra, Dharug, Yengo

Figure 3: Connectivity Examples

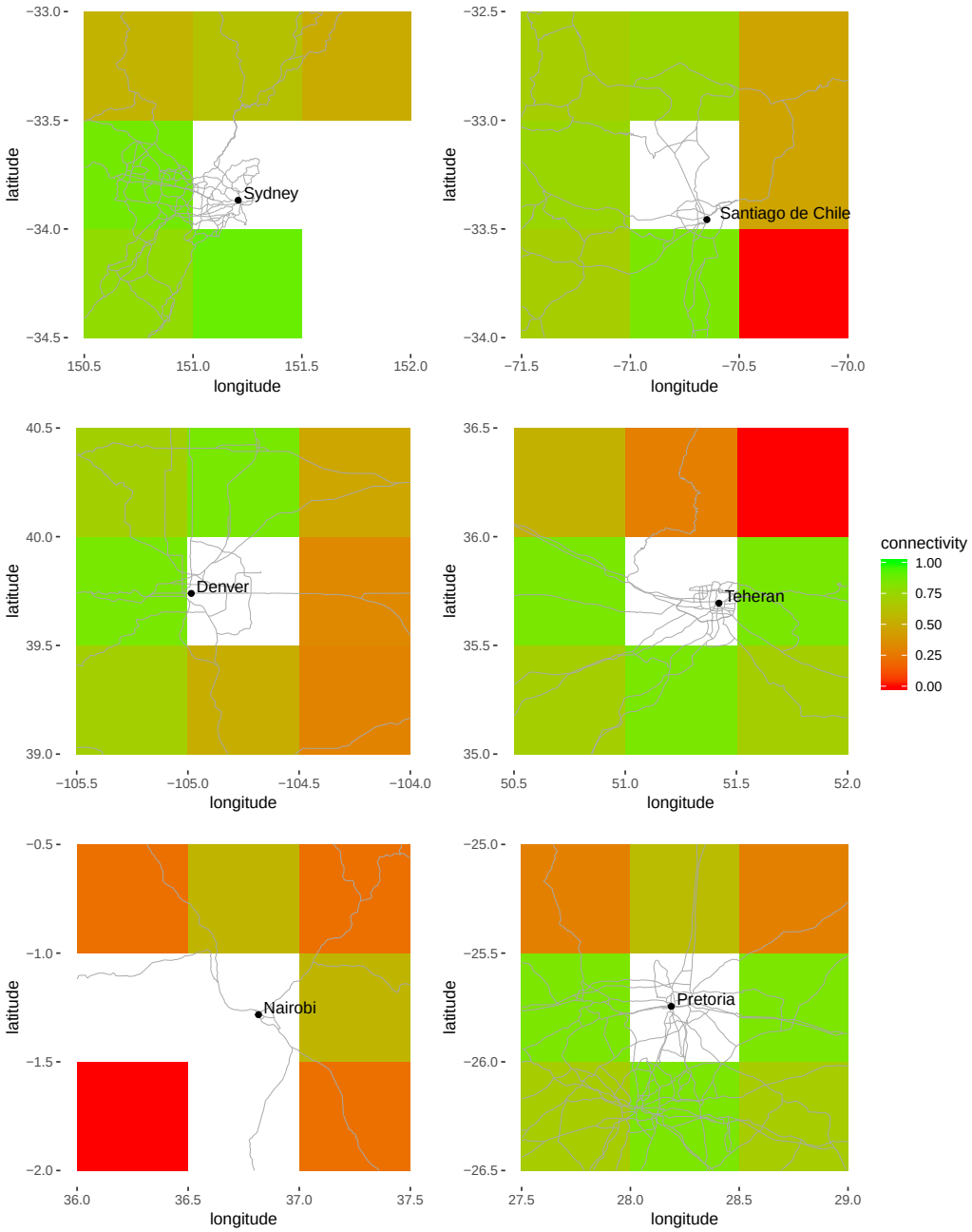

Note: Sources: Esri, Garmin International, Inc., own calculations. Connectivity increases along red-green spectrum with bright green representing the highest level of the connectivity index. Transparent cells are excluded from the balanced panel due to lack of night-time light emission data (usually hinterland, desert or on-sea locations).

and Wollemi National Parks which impose limitations on road access. For Santiago de Chile, the tightest connections exist with cells in the immediate South including parts of the city and the connected towns of San Bernardo and Puente Alto. Western cells are also

well connected, with many small towns and linking Santiago de Chile to the seaside cities San Antonio, Valparaíso and Viña del Mar. To the East starts the Andean mountain range, connectivity is thus relatively low. For Denver on the other hand the link to the Rocky Mountains in the West, an economically important area during the Colorado gold rush in the 19th century, is much more pronounced than connections leading into the Great Plains to the East. To provide an example from the Middle East, Teheran is well-connected to the South, East and West. In the North, it adjoins the Varjin Protected Area crossed exclusively by Chalus Road (visible in the top middle cell) which connects Teheran to the Caspian Sea. Finally, Nairobi and Pretoria serve to demonstrate the vast heterogeneity in terms of connectivity when we compare two African capital cities. While Pretoria is well connected, especially to the economic center of Johannesburg in the South, Nairobi features a less developed roads infrastructure and even contains two cells for which no economic activity is reflected in the night-lights data.

Overall, corner cells tend to show a lower connectivity value than directly adjacent cells simply due to overall longer average distances along the diagonal. Descriptives indicate that the connectivity index is capable of generating plausible patterns in line with natural geographic features. We thus consider it an adequate proxy for the true connectedness of locations.

3. Empirical Strategy

To study the relation between severe weather and economic growth, we apply a macroeconomic growth model following Islam (1995) and Acemoglu et al. (2005). We take a granular approach and account for the spatial dependence of our data to avoid omitted variable bias. Hence, we adopt a modified spatial Durbin error model (SDEM) with cell and year fixed effects[13]

$$\Delta \boldsymbol{\ell_t} = \boldsymbol{\ell_{t-1}}\gamma + \boldsymbol{D_t}\boldsymbol{\beta^0} + \sum_{i}^{k} (\boldsymbol{C^i} \odot \boldsymbol{W^r})\boldsymbol{D_t}\boldsymbol{\beta^i} + \boldsymbol{X_t}\boldsymbol{\delta^0} + \boldsymbol{W^r}\boldsymbol{X_t}\boldsymbol{\delta^1} + \boldsymbol{\nu} + \boldsymbol{\pi} + \boldsymbol{u_t} \quad (3)$$

$$\boldsymbol{u_t} = \rho \boldsymbol{W^r}\boldsymbol{u_t} + \boldsymbol{\varepsilon_t}$$

where $\Delta\boldsymbol{\ell_t}$ is a proxy for cell economic growth rates, measured by annual changes in the log of mean night-light emissions $\Delta\boldsymbol{\ell_t} \equiv \ln\left(\overline{\mathbf{light}_t}\right) - \ln\left(\overline{\mathbf{light}_{t-1}}\right)$. $\boldsymbol{D_t}$ represents

[13]See Anselin (2013) and Halleck Vega and Elhorst (2015) for a detailed description of the standard SDEM.

weather events and $\boldsymbol{X_t}$ contains controls. $\boldsymbol{\nu}$ is a vector of cell fixed effects and controls for time-constant local unobservables.[14] $\boldsymbol{\nu}$ takes out the location-specific baseline risk of unexpected weather events. It also controls for structural determinants of the relationship between light use and GDP growth, such as political, cultural, historical and geographic fundamentals. $\boldsymbol{\pi}$ represents time fixed effects. These capture unobserved global characteristics, such as technological progress and the global business cycles, but also control for systematic variation in the measurement of light emissions over time, see Henderson et al. (2012).[15]

$\boldsymbol{W^r}$ is a time-invariant $K \times K$ dimension spatial weights matrix with binary elements. As recommended by Conley (2008), it contains all units within a spatial radius r around a given location.[16] To ensure that a neighborhood's area size does not vary systematically across latitude, we choose a constant metric radius r. We set r to 80 km, this matches eight adjacent cells at the equator.[17] To test whether spillover effects are transmitted via a specific connectivity channel, we construct a set of k connectivity matrices $\boldsymbol{C^i}$, $i \in k$. Each matrix consists of binary elements assigning a weight of one to all units satisfying a defined connectivity criterion and zero otherwise.[18] We then multiply each connectivity matrix with $\boldsymbol{W^r}$, such that $\boldsymbol{C^i} \odot \boldsymbol{W^r}$ provides a combined filter which extracts groups of neighbors within radius r satisfying a common connectivity criterion i. Multiplying weather events with this filter produces group-specific spatial lags. $\boldsymbol{\beta^i}$ gives the average local spillover effect of a marginal change in the weather measure in *one* neighboring cell that falls into a given group i. Note that the matrix multiplications for spillover terms produce sums over particular groups. This has two implications: First, identification along a quasi diff-in-diff specification is econometrically unfeasible as exogenous treatment of different neighboring groups might jointly affect the outcome of the *same* observational unit. We take this into account by explicitly treating different neighboring groups as separate explanatory factors of the same outcome. Second, the sums over different groups

[14] It accounts for systematic measurement error in night lights due to aurora, the solar cycle, and stray light.

[15] The capacity of satellite sensors varies systematically as they erode over time or are replaced by newer models. Elvidge et al. (2009, 2014) propose to inter-calibrate the original pixel data by normalizing all values to a base year for a reference area. Contrary, fixed effects require no assumptions on the stability of lights in any temporal or spatial window.

[16] This implies that the same set of neighbors must be used for each cell throughout the analysis, i.e., the panel must be balanced.

[17] Previous research has shown that natural disasters are rather local phenomenon (cf. Strobl, 2011; Bertinelli and Strobl, 2013; Elliott et al., 2015).

[18] Each matrix is mutually exclusive and collectively exhaustive relative to the universe of neighboring cells defined by $\boldsymbol{W^r}$.

of neighboring cells may follow different distributions. We compute z-scores to compare magnitudes directly within the vector $\boldsymbol{\beta^i}$.

Note that entries in the connectivity matrix $\boldsymbol{C^i}$ may be endogenous, e.g., road connectivity. We account for this by using cell fixed effects, which absorb all unobservable cell-specific links between light emission and connectivity. Moreover, we are interested not in $\boldsymbol{C^i}$ itself, but in its interaction with the weather event. Nizalova and Murtazashvili (2016) and Beverelli et al. (2018) show that potential endogeneity vanishes upon interaction with an exogenous variable. As we multiply $\boldsymbol{C^i}$ with physical weather intensities, estimates are consistent if weather events are uncorrelated with the elements of $\boldsymbol{C^i}$ or potential omitted variables. Finally, $\boldsymbol{u_t}$ allows for spatial auto-correlation in residuals. Hence, we account for spatial clustering and spillovers in unobserved characteristics. Such patterns potentially result from the fact that superimposed grid cells arbitrarily intersect true economic units such that adjacent cells share common business cycles or institutions.

4. Results

Next, we explore whether connectivity – measured by national borders and road networks – acts as a transmission channel of severe weather in small economic units.

4.1. International Borders

Geography plays a significant role in shaping economic outcomes and national borders particularly influence political, economical and cultural factors. While power usually stays within sovereign boundaries, institutional differences between countries may have strong economic implications (Acemoglu et al., 2005). Further, the physical distance between two observational units reduces the amount of economic transactions between them (McCallum, 1995; Obstfeld and Rogoff, 2000; Anderson and Van Wincoop, 2003). National borders thus constitute barriers to the flow of goods, information, finance, and people (Helliwell, 1997; Helliwell and McKitrick, 1999; Helliwell, 2000; Helliwell and Verdier, 2001; Helliwell, 2002; Anderson and Van Wincoop, 2004; Chen, 2004). They may lead to the fragmentation of production as the connectivity of international markets and border efficiency play an important role (World Bank, 2019). While economic ties within nations are typically stronger than international economic links – even with preceding globalization –, national economies have a strong staying power. This in mind, we explore whether international borders lead to localized spillover effects of weather events in the short-run. For this purpose, connectivity is defined as $\sum_i^k \boldsymbol{C^i} = \boldsymbol{C}^{\text{same}} + \boldsymbol{C}^{\text{diff}}$, where $\boldsymbol{C}^{\text{same}}$ assigns

a weight of one to all cells belonging to the same country while $\boldsymbol{C}^{\text{diff}}$ assigns a weight of one to those in a different country.

Table 1: Border Effect

Dependent Variable: $\Delta \ln(\text{lights}_t)$

	wind	**precip.**	**cold**
event_t	-0.0048^{***}	-0.0295^{***}	-0.0562^{***}
	(0.0009)	(0.0069)	(0.0133)
$C^{\text{same}} \odot W^r \cdot \text{event}_t$	0.0405^{***}	0.0071^{***}	0.0240^{***}
	(0.0099)	(0.0019)	(0.0030)
$C^{\text{diff}} \odot W^r \cdot \text{event}_t$	-0.0006	-0.0005	0.0162^{***}
	(0.0100)	(0.0016)	(0.0034)
$\ln(\text{pop}_t)$	0.0247^{***}	0.0257^{***}	0.0243^{***}
	(0.0013)	(0.0013)	(0.0013)
$W^r \cdot \ln(\text{pop})_t$	0.0109^{***}	0.0112^{***}	0.0106^{***}
	(0.0006)	(0.0006)	(0.0006)
$\ln(\text{lights}_{t-1})$	-0.4387^{***}	-0.4367^{***}	-0.4380^{***}
	(0.0011)	(0.0011)	(0.0011)
Observations	507,864	502,026	506,037
Wald $\boldsymbol{\chi^2}$ H0: Spillover from $\boldsymbol{C}^{\text{same}}$ = Spillover from $\boldsymbol{C}^{\text{diff}}$			
$\Pr(> \chi^2)$	0.0008^{***}	0.0004^{***}	0.0492^{**}

Note: ***, **, * denote significance at the 1%, 5% and 10% level. All specifications are SDEM and are estimated by Maximum Likelihood. Standard errors in parentheses. Cell and year fixed effects, and first temporal lags of weather events included but not reported. Spatial radius is r=80 km. Yearly disaster intensities reflect time-weighted rolling averages over 12 subsequent monthly observations. $C^i \odot W^r \cdot \text{event}_t$ terms represent corresponding z-scores.

Table 1 shows that wind speeds, extreme precipitation and cold waves have negative local effects on the growth rate of night-light emissions – a proxy of economic activity. Reported winds lead on average to a 0.5 percentage points reduction in economic growth, excessive rain anomalies reduce growth in economic activity by 3.0 percentage points and cold waves by 5.6 percentage points over 12 months following the event.[19] Economic diversion is exclusively driven by domestic cells for wind and precipitation events. For cold waves, domestic relocation shows significantly stronger effects than foreign cells, with

[19]We take definitions of the physical intensity of weather events from the GAME database described in Felbermayr et al. (2018).

magnitudes about 1.5 times the size.[20] Hence, the diversion of economic activity with severe weather happens mostly (if not exclusively) through substitution effects to domestic neighbors.[21] This provides evidence that, at least in the short-run, regional economic linkages are stronger than international ones. It also supports the fact that domestic linkages are more efficient and resilient, while international connectivity is subject to higher costs, lower speed, and higher uncertainty, see World Bank (2019). Control variables are as expected. Population size and their neighbors add to the growth of economic activity, while the lag of light is negatively correlated with the dependent variable.

4.2. Road Existence

Whereas distance and geography are fixed, connectivity might be subject to change. Transport networks, particularly the availability of highways, provide a potential mediating factor (Banerjee et al., 2012; Faber, 2014). But, the effective establishment of economic linkages depends not only on the existence of transport routes but also on the reliability of road infrastructure (cf. World Bank, 2019). We thus assess the role of the general availability of roads to examine whether spillovers from neighboring units connected by road are stronger than those without a connection – the latter being in general more costly. For about one fifth of our balanced sample the data show no major roads connection to adjacent cells, even though locations may still exhibit substantial economic activity, compare Figure 2b. To explore whether the availability of major roads plays a significant role in the transmission of weather effects[22], we define connectivity as $\sum_i^k \boldsymbol{C^i} = \boldsymbol{C}^{\text{roads}} + \boldsymbol{C}^{\text{no-roads}}$, where $\boldsymbol{C}^{\text{roads}}$ assigns a weight of one to all neighbors connected by at least one road and $\boldsymbol{C}^{\text{no-roads}}$ captures neighbors that lack a connection.

Table 2 presents results. Control variables and direct effects of weather events show similar results to the previous analysis, albeit with a loss of statistical significance for winds. Results on spillovers strongly indicate that the availability of road infrastructure is a key driver of the diversion of economic activity across space in the case of severe weather. For wind speeds, we find no statistically significant direct or spillover effects. Estimates

[20] Wald chi-squared tests suggest that the similarity of spillover effects from domestic and foreign cells is overwhelmingly rejected for all types of events.

[21] Over longer periods, country borders may be overcome by international adaption activities. International relocation of activity takes time as cross-border transactions (i.e., international trade or migration) are subject to bureaucratic and knowledge constraints that do not or to a lesser extent apply to domestic relocation.

[22] Even in the absence of observed roads, effects from weather events could be transmitted via roads, navigable waterways or railways not captured by the data. Unfortunately, the two latter sources of connectivity are beyond the scope of this paper and left for future research.

Table 2: Road Existence

Dependent Variable: $\Delta \ln(\text{lights}_t)$

	wind	**precip.**	**cold**
event_t	−0.0012	−0.0301***	−0.0338**
	(0.0009)	(0.0069)	(0.0146)
$C^{\text{roads}} \odot W^r \cdot \text{event}_t$	−0.0125	0.0106***	0.0280***
	(0.0124)	(0.0021)	(0.0041)
$C^{\text{no-roads}} \odot W^r \cdot \text{event}_t$	−0.0086	0.0008	0.0080**
	(0.0120)	(0.0019)	(0.0040)
$\ln(\text{pop}_t)$	0.0249***	0.0258***	0.0244***
	(0.0013)	(0.0013)	(0.0013)
$W^r \cdot \ln(\text{pop})_t$	0.0109***	0.0113***	0.0106***
	(0.0006)	(0.0006)	(0.0006)
$\ln(\text{lights}_{t-1})$	−0.4386***	−0.4368***	−0.4380***
	(0.0011)	(0.0011)	(0.0011)
Observations	507,864	502,026	506,037
Wald χ^2 H0: Spillover from C^{roads} = Spillover from $C^{\text{no-roads}}$			
$\Pr(>\chi^2)$	0.7220	0.0000***	0.0000***

Note: ***, **, * denote significance at the 1%, 5% and 10% level. All specifications are SDEM and are estimated by Maximum Likelihood. Standard errors in parentheses. Cell and year fixed effects, and first temporal lags of weather events included but not reported. Spatial radius is r=80 km. Yearly disaster intensities reflect time-weighted rolling averages over 12 subsequent monthly observations. $C^i \odot W^r \cdot \text{event}_t$ terms represent corresponding z-scores.

on extreme precipitation suggest that economic relocation is driven exclusively through neighboring locations that are connected by roads. For cold waves, both connected and unconnected cells hold diversion patterns. Therein, connected neighbors account for more than three times the magnitude of those from unconnected cells. As before, Wald chi-squared tests reject the similarity of spillover effects from connected and unconnected cells. Hence, the existence of road infrastructure between locations is key to economic relocation of goods or people in the case of severe weather. Without a transport network, diversion between local units does not happen, or is at least limited and rather costly.

4.3. Road Heterogeneity

Next, we explore the role of infrastructure through the quantity and distance of road connections. We use the distribution of road connectivity to investigate whether a better connectivity of locations eases the diversion of economic activity upon weather events. With more infrastructure available, economic ties between locations are likely to be more

tight, routing of economic exchange is less costly and can be diverted more easily if one connection is blocked or congested. As described in Section 2.3, the connectivity measure increases in inverse distance and in the number of up to three independent road connections.[23]

We start by classifying neighboring cells into bins along a relative notion of local connectivity. With a global or regional (beyond local) reference value, we run the risk of capturing regional differences in the spillover estimates due to unobserved characteristics rather than informing about the role of roads. Cells from highly connected locations (e.g., Western Europe or the U.S. East Coast) which also stand out due to other characteristics that are potentially correlated with roads infrastructure may effectively be over-represented in chosen connectivity categories. To circumvent this, we chose connectivity classes such that bins capture adjacent cells by their relative connectivity compared to cells within the same local neighborhood.[24] First, we consider two bins that divide neighbors into high and low connected cells, $\sum_i^k \boldsymbol{C^i} = \boldsymbol{C}^{\text{high}} + \boldsymbol{C}^{\text{low}}$. The splitting criterion is the median of the local distribution, which ensures that each group is represented for an observational unit and that both groups are approximately equal in size.[25]

Table 3 Panel A presents results. Estimates of weather events are negative, statistically significant and in line with magnitudes obtained from previous specifications. For precipitation and cold events, spillover estimates are stronger from highly connected neighbors compared to those from cells with a connectivity below the local median. We find no statistically significant effects on relocation effects of connectivity for storms. Again, Wald Chi-Squared tests show that similarity of spillovers is rejected, see Table A4 in the Appendix. This confirms that relocation across highly connected neighbors are stronger than transactions across worse connections, which are much more expensive to implement.

Second, we distinguish high, medium and low connected cells, $\sum_i^k \boldsymbol{C^i} = \boldsymbol{C}^{\text{high}} + \boldsymbol{C}^{\text{medium}} + \boldsymbol{C}^{\text{low}}$. These are selected along the thirtiles of the local neighborhoods' connectivity distributions. Results are presented in Panel B of Table 3. Again, we cannot distinguish any relocation effects for storms. For remaining weather events, we observe a mixed spillover pattern. We find a clear hierarchy for extreme precipitation with spillover magnitudes gradually declining from high to middle to low connectivity neighbors. Re-

[23]The algorithm searches for the three shortest routes and adds a penalty if less routes exist. Note that this choice is arbitrary. We relax the criterion in the sensitivity analysis considering only the length of the single shortest connection.

[24]A neighboring location which is badly connected overall could still be relatively important for the spillover mechanism, if other nearby places feature connections that are even worse.

[25]Cells that have a connectivity which is exactly equal to the median are classified as highly connected. If all cells within a neighborhood have a connectivity index of zero, these are defined as low connections. The robustness section 5.1 provides estimates using the local mean instead.

Table 3: Road Heterogeneity

Dependent Variable: $\Delta \ln(\text{lights}_t)$

	wind	**precip.**	**cold**
PANEL A: Connectivity Above and Below Median			
event_t	−0.0025***	−0.0277***	−0.0432***
	(0.0009)	(0.0069)	(0.0141)
$C^{\text{high}} \odot W^r \cdot \text{event}_t$	−0.0051	0.0074***	0.0213***
	(0.0088)	(0.0015)	(0.0028)
$C^{\text{low}} \odot W^r \cdot \text{event}_t$	0.0141	0.0012	0.0102***
	(0.0087)	(0.0015)	(0.0029)
PANEL B: Connectivity Thirtiles			
event_t	−0.0015*	−0.0266***	−0.0350**
	(0.0009)	(0.0069)	(0.0145)
$C^{\text{high}} \odot W^r \cdot \text{event}_t$	−0.0017	0.0057***	0.0113***
	(0.0089)	(0.0015)	(0.0031)
$C^{\text{medium}} \odot W^r \cdot \text{event}_t$	−0.0072	0.0031**	0.0130***
	(0.0090)	(0.0015)	(0.0032)
$C^{\text{low}} \odot W^r \cdot \text{event}_t$	−0.0018	0.0005	0.0086***
	(0.0090)	(0.0015)	(0.0030)
Observations	507,864	502,026	506,037

Note: ***, **, * denote significance at the 1%, 5% and 10% level. All specifications are SDEM and are estimated by Maximum Likelihood. Standard errors in parentheses. Cell and year fixed effects, and first temporal lags of weather events included but not reported. Spatial radius is r=80 km. Yearly disaster intensities reflect time-weighted rolling averages over 12 subsequent monthly observations. $C^i \odot W^r \cdot \text{event}_t$ terms represent corresponding z-scores. Full results are shown in Tables A2 and A3 in the Appendix.

location due to cold waves are weakest for low connected cells, but of similar magnitude for cells with a high and middle connectivity.[26]

5. Robustness Analysis

This section performs a number of robustness checks. First, we alter the splitting criterion to assess the connection of cells. Second, we use the length of the single shortest path. Finally, we remove observations with insufficient local neighbors.

5.1. The Local Mean as Splitting Criterion

In the baseline, we use the median connectivity within the local neighborhood as a cutoff criterion to separate the top half of neighboring observations from the bottom half. This

[26]While the point estimate is larger for units with a medium compared to high connectivity, the difference is not statistically significant. See Wald Chi-Squared tests in Table A5.

has the advantage that both neighboring groups are approximately equal in size. To check whether results are sensitive to the definition of this reference criterion, we replace the local median by the local arithmetic mean. Table 4 Panel A shows that all estimates remain qualitatively similar to previous findings. Consequently, estimates are robust to the exact definition of the connectivity cutoff criterion.

5.2. The Shortest Connection

The baseline indicator accounts for both distance and the number of connections. We reconsider this choice and use only the distance along the single shortest route. This potentially affects the position of a cell within the local connectivity distribution and may thus result in different binning outcomes. Table 4, Panel B and Panel C show that estimates remain qualitatively similar. In Panel B, magnitudes on weather events show slightly higher point estimates for transmissions from highly connected cells and smaller effects for lowly connected neighbors. Hence, the importance of above-median relative to below-median connections increases if only the shortest route is considered, i.e., distance is more important than the number of connections. If we distinguish three categories in Panel C, we find some significant differences for precipitation events. Relocation effects from intermediately connected cells lose statistical significance, attributing all spillovers to highly connected neighbors. For cold waves, the highest connected neighbors now show the strongest effects. Again, results suggest that distance between economic units is more important than the number of roads connecting the cells.

5.3. Exclude Observations With Less Than Three Neighbors

Further, we explore how the distance and the number of road connections between cells affect the relocation of economic activity due to severe weather by excluding observations with less than three neighboring cells. As our approach requires the construction of multiple bins along the local distribution of road connectivity, the number of adjacent cells matters. If a cell has only one neighbor and this neighbor has a connectivity of zero, then it will always fall into the low connectivity group, while the group of highly connected cells is zero.[27] Hence, the sample includes observations for which some groups are zero by construction, simply because there are no reference cells. To assess whether this feature entails identification issues, we drop all observations with less than three neighbors from

[27]Assume that the same neighbor has a non-zero connectivity, the splitting criterion along the local median will put it into the highly connected category instead.

the sample.[28] These observations account for about 10% of the sample. Table 4 Panel D provides estimates for groups split along the median, Panel E distinguishes three groups (high, medium and low). Findings are qualitatively robust. Hence, the inclusion of cells with a very small number of neighbors does not substantially affect our results.[29]

6. Conclusion

This paper studies how the economic effects of severe weather transmit between locations. We are particularly interested in the role of the interconnection of random small economic units. We ask how the spillover of economic activity is affected by international borders and by available road infrastructure. To answer this question, we combine grid-cell level data on the physical intensity of weather and remotely-sensed night-light emissions – a proxy for local economic activity – with global geographic information on national borders and major road networks. As the connectivity of economic units is a multi-layer concept, we first explore how a disruption of connectivity through an international border limits local spillovers in the case of extreme weather. Country boundaries constitute frictions to the diversion of goods, information, financial flows, and people and are expected to contain the economic effects of weather events within regions. Second, we use the transportation system as a proxy for overall connectivity to explore whether infrastructure promotes the relocation of economic activity across small economic units with extreme weather. As spillovers from weather events are likely to be driven by the degree of connectivity between locations, we expect that available roads strengthen relocation effects.

Our findings support that severe weather generally hampers the growth of local economic activity. Results suggest that the connectivity of cells is a main driver of economic relocation from weather events. For national borders, we find increased localization and a fragmentation of production across countries. Domestic cells are, on average, the exclusive sources of diversion for wind and precipitation events. For cold waves, domestic relocation shows 1.5 times stronger effects than foreign cells. Hence, economic diversion in the case of extreme weather happens mostly (if not exclusively) through substitution effects to domestic neighbors. This supports that domestic linkages are generally more efficient and resilient, while international connectivity is subject to higher costs, lower speed, and higher uncertainty. Further, we explore the impact of the existence of road

[28] This removes cells for small islands or otherwise remote locations, which are more likely to appear in less developed countries, see Figure 1.

[29] Appendix Tables A8 and A9 provide additional estimates for a sample excluding observations with less than two neighbors. Results are robust.

infrastructure, as connectivity along major transport routes potentially eases travel time and reduces transport costs. Results indicate that the availability of at least one major road exclusively drives the diversion of economic activity for extreme precipitation events. For cold waves, economic relocation effects are 3.5 times as strong for connected compared to unconnected neighboring cells. Finally, with more available infrastructure, economic ties between locations are likely to be more tight and routing of economic exchange can be diverted more easily if a connection is blocked or congested. For precipitation and cold events, estimates confirm that relocation across highly connected neighbors are stronger than transactions across worse and thus more costly connections.

Overall, our findings suggest that international borders contain economic relocation activity due to weather events within the local domestic neighborhood. Then again, the existence of major road infrastructure between locations is key to economic relocation of goods or people under extreme weather. Without a transport network, spillovers between local economic units do, on average, not exist or are at least very limited and much more costly to implement. Yet, the ability to divert economic activity helps to mitigate the effects of extreme weather events and build resilience against potential future events.

Table 4: Robustness

Dependent Variable: $\Delta \ln(\text{lights}_t)$

	wind	**precip.**	**cold**
PANEL A: Connectivity along Local Mean			
event_t	−0.0025***	−0.0276***	−0.0471***
	(0.0009)	(0.0069)	(0.0143)
$C^{\text{high}} \odot W^r \cdot \text{event}_t$	−0.0056	0.0069***	0.0201***
	(0.0090)	(0.0015)	(0.0029)
$C^{\text{low}} \odot W^r \cdot \text{event}_t$	0.0145	0.0020	0.0143***
	(0.0089)	(0.0015)	(0.0030)
PANEL B: Shortest Road Connection (Median)			
event_t	−0.0025***	−0.0280***	−0.0410***
	(0.0009)	(0.0069)	(0.0141)
$C^{\text{high}} \odot W^r \cdot \text{event}_t$	−0.0039	0.0082***	0.0221***
	(0.0090)	(0.0015)	(0.0029)
$C^{\text{low}} \odot W^r \cdot \text{event}_t$	0.0128	0.0006	0.0091***
	(0.0088)	(0.0015)	(0.0029)
PANEL C: Shortest Road Connection (Thirtiles)			
event_t	−0.0016*	−0.0275***	−0.0355**
	(0.0009)	(0.0070)	(0.0144)
$C^{\text{high}} \odot W^r \cdot \text{event}_t$	−0.0060	0.0064***	0.0150***
	(0.0104)	(0.0017)	(0.0036)
$C^{\text{medium}} \odot W^r \cdot \text{event}_t$	0.0006	0.0021	0.0082**
	(0.0105)	(0.0017)	(0.0038)
$C^{\text{low}} \odot W^r \cdot \text{event}_t$	−0.0015	0.0006	0.0085***
	(0.0090)	(0.0015)	(0.0030)
PANEL D: Exclude Cells with <3 Neighbors (Median)			
event_t	−0.0025**	−0.0211***	−0.0738***
	(0.0011)	(0.0080)	(0.0184)
$C^{\text{high}} \odot W^r \cdot \text{event}_t$	−0.0078	0.0060***	0.0241***
	(0.0089)	(0.0015)	(0.0030)
$C^{\text{low}} \odot W^r \cdot \text{event}_t$	0.0099	0.0006	0.0134***
	(0.0088)	(0.0016)	(0.0030)
PANEL E: Exclude Cells with <3 Neighbors (Thirtiles)			
event_t	−0.0009	−0.0211***	−0.0583***
	(0.0011)	(0.0080)	(0.0189)
$C^{\text{high}} \odot W^r \cdot \text{event}_t$	−0.0071	0.0045***	0.0121***
	(0.0087)	(0.0015)	(0.0031)
$C^{\text{medium}} \odot W^r \cdot \text{event}_t$	−0.0095	0.0029*	0.0155***
	(0.0088)	(0.0015)	(0.0032)
$C^{\text{low}} \odot W^r \cdot \text{event}_t$	−0.0085	0.0002	0.0110***
	(0.0093)	(0.0016)	(0.0033)

Note: ***, **, * denote significance at the 1%, 5% and 10% level. All specifications are SDEM and are estimated by Maximum Likelihood. Standard errors in parentheses. Cell and year fixed effects, and first temporal lags of weather events included but not reported. Spatial radius is r=80 km. Yearly disaster intensities reflect time-weighted rolling averages over 12 subsequent monthly observations. Full results are shown in Tables A6 and A7 in the Appendix.

References

Acemoglu, D., Johnson, S., Robinson, J. A., 2005. Institutions as a Fundamental Cause of Long-Run Growth. in: Aghion, P. and Durlauf, S. (eds.), Handbook of Economic Growth 1, 385–472.

Amarasinghe, A., Hodler, R., Raschky, P. A., Zenou, Y., April 2018. Spatial Diffusion of Economic Shocks in Networks. CESifo Working Paper 7001, CESifo Group Munich.

Anderson, J. E., Van Wincoop, E., 2003. Gravity with Gravitas: A Solution to the Border Puzzle. American Economic Review 93 (1), 170–192.

Anderson, J. E., Van Wincoop, E., 2004. Trade Costs. Journal of Economic Literature 42 (3), 691–751.

Anselin, L., 2013. Spatial Econometrics: Methods and Models. Vol. 4. Springer Science & Business Media.

Banerjee, A., Duflo, E., Qian, N., 2012. On the road: Access to transportation infrastructure and economic growth in china. Tech. rep., National Bureau of Economic Research.

Bertinelli, L., Strobl, E., 2013. Quantifying the Local Economic Growth Impact of Hurricane Strikes: An Analysis from Outer Space for the Caribbean. Journal of Applied Meteorology and Climatology 52 (8), 1688–1697.

Beverelli, C., Keck, A., Larch, M., Yotov, Y. V., February 2018. Institutions, Trade and Development: A Quantitative Analysis. CESifo Working Paper 6920, CESifo Group Munich.

Buchan, N., Fatas, E., Grimalda, G., 2012. Connectivity and Cooperation. The Oxford Handbook of Economic Conflict Resolution. New York: Oxford University Press Inc, 155–79.

Burke, M., Emerick, K., 2016. Adaptation to Climate Change: Evidence from US Agriculture. American Economic Journal: Economic Policy 8 (3), 106–40.

Cavallo, E., Noy, I., 2011. Natural Disasters and the Economy A Survey. International Review of Environmental and Resource Economics 5 (1), 63–102.

Chen, N., 2004. Intra-National Versus International Trade in the European Union: Why Do National Borders Matter? Journal of International Economics 63 (1), 93–118.

Conley, T. G., 2008. Spatial Econometrics. Palgrave Macmillan.

Costinot, A., Donaldson, D., Smith, C., 2016. Evolving Comparative Advantage and the Impact of Climate Change in Agricultural Markets: Evidence from 1.7 Million Fields Around the World. Journal of Political Economy 124 (1), 205–248.

Deschênes, O., Greenstone, M., 2012. The Economic Impacts of Climate Change: Evidence from Agricultural Output and Random Fluctuations in Weather: Reply. American Economic Review 102 (7), 3761–3773.

Desmet, K., Rossi-Hansberg, E., 2015. On the Spatial Economic Impact of Global Warming. Journal of Urban Economics 88, 16–37.

Dijkstra, E. W., 1959. A Note on Two Problems in Connexion with Graphs. Numerische Mathematik 1, 269–271.

Elliott, R., Strobl, E., Sun, P., 2015. The Local Impact of Typhoons on Economic Activity in China: A View from Outer Space. Journal of Urban Economics 88, 50–66.

Elvidge, C. D., Hsu, F.-C., Baugh, K. E., Ghosh, T., 2014. National Trends in Satellite Observed Lighting. Global Urban Monitoring and Assessment through Earth Observation 23, 97–118.

Elvidge, C. D., Ziskin, D., Baugh, K. E., Tuttle, B. T., Ghosh, T., Pack, D. W., Erwin, E. H., Zhizhin, M., 2009. A Fifteen Year Record of Global Natural Gas Flaring Derived from Satellite Data. Energies 2 (3), 595–622.

Environmental Systems Research Institute, 2016. Data and Maps for ARCGIS, 2016 - World, Europe, and United States: World Roads.

Faber, B., 2014. Trade integration, market size, and industrialization: evidence from china's national trunk highway system. Review of Economic Studies 81 (3), 1046–1070.

Felbermayr, G., Gröschl, J., 2014. Naturally Negative: The Growth Effects of Natural Disasters. Journal of Development Economics 111, 92–106.

Felbermayr, G., Gröschl, J. K., Sanders, M., Schippers, V., Steinwachs, T., July 2018. Shedding light on the spatial diffusion of disasters. CESifo Working Paper 7146, CESifo Group Munich.

Fisher, A. C., Hanemann, W. M., Roberts, M. J., Schlenker, W., 2012. The Economic Impacts of Climate Change: Evidence From Agricultural Output and Random Fluctuations in Weather: Comment. American Economic Review 102 (7), 3749–3760.

Halleck Vega, S., Elhorst, J. P., 2015. The SLX Model. Journal of Regional Science 55 (3), 339–363.

Helliwell, J. F., 1997. National borders, trade and migration. Pacific Economic Review 2 (3), 165–185.

Helliwell, J. F., 2000. How Much Do National Borders Matter? Brookings Institution Press.

Helliwell, J. F., 2002. Measuring the Width of National Borders. Review of International Economics 10 (3), 517–524.

Helliwell, J. F., McKitrick, R., 1999. Comparing Capital Mobility Across Provincial And National Borders. Canadian Journal of Economics, 1164–1173.

Helliwell, J. F., Verdier, G., 2001. Measuring Internal Trade Distances: A New Method Applied to Estimate Provincial Border Effects in Canada. Canadian Journal of Economics, 1024–1041.

Henderson, J. V., Squires, T., Storeygard, A., Weil, D., 2017. The Global Distribution of Economic Activity: Nature, History, and the Role of Trade. Quarterly Journal of Economics 133 (1), 357–406.

Henderson, J. V., Storeygard, A., Weil, D. N., 2012. Measuring Economic Growth from Outer Space. American Economic Review 102 (2), 994–1028.

Hsieh, C.-T., Ossa, R., 2016. A Global View of Productivity Growth in China. Journal of International Economics 102, 209–224.

Islam, N., 1995. Growth Empirics: A Panel Data Approach. Quarterly Journal of Economics 110 (4), 1127–1170.

McCallum, J., 1995. National Borders Matter: Canada-US Regional Trade Patterns. American Economic Review 85 (3), 615–623.

Nizalova, O. Y., Murtazashvili, I., 2016. Exogenous Treatment and Endogenous Factors: Vanishing of Omitted Variable Bias on the Interaction Term. Journal of Econometric Methods 5 (1), 71–77.

Nordhaus, W. D., Chen, X., 2009. Geography: Graphics and Economics. The BE Journal of Economic Analysis & Policy 9 (2).

Noy, I., 2009. The Macroeconomic Consequences of Disasters. Journal of Development Economics 88 (2), 221–231.

Obstfeld, M., Rogoff, K., 2000. The Six Major Puzzles in International Macroeconomics: Is There a Common Cause? NBER Macroeconomics Annual 15, 339–390.

Storeygard, A., 2016. Farther on Down the Road: Transport Costs, Trade and Urban Growth in Sub-Saharan Africa. Review of Economic Studies 83 (3), 1263–1295.

Strobl, E., 2011. The Economic Growth Impact of Hurricanes: Evidence from US Coastal Counties. Review of Economics and Statistics 93 (2), 575–589.

World Bank, January 2019. Infrastructure Connectivity. Tech. rep., G20 Background Paper.

A. Appendix

Table A1: Summary Statistics

statistic	n	mean	st. dev.	min	max
$\Delta \ln(\text{lights})$	507,864	0.045	0.392	−8.246	8.217
$\ln(\text{lights})$	507,864	0.264	1.724	−7.090	4.142
$\ln(\text{pop}_t)$	507,864	10.639	2.165	−14.390	16.822
Physical Intensities					
storm	507,864	20.766	4.486	5.478	46.528
precip.	502,026	0.385	0.151	0.000	1.697
cold	506,037	0.412	0.089	0.000	1.271
Roads Connectivity Index (cross-section)					
bilat. connectivity (3 routes)	169,626	0.326	0.230	0.000	0.913
mean connectivity (3 routes)	24,184	0.301	0.233	0.000	0.873
bilat. connectivity (1 route)	169,626	0.526	0.357	0.000	0.916
mean connectivity (1 route)	24,184	0.501	0.293	0.000	0.914

Note: Physical intensities represent time-weighted rolling averages over 12 subsequent months. Time-constant connectivity measures are reported for one year. 21 yearly periods included in the data.

Figure A1: Connectivity vs. Activity

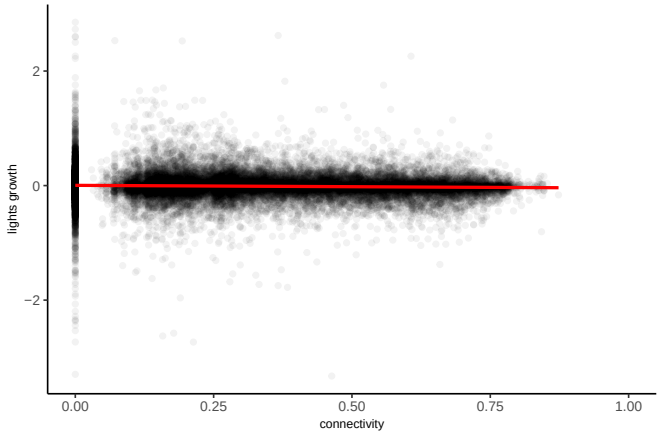

Note: Plotted lights growth represent absolute growth values in 2013.

Table A2: Roads Connectivity Above And Below Median

Dependent Variable: $\Delta \ln(\text{lights}_t)$

	wind	**precip.**	**cold**
event_t	-0.0025^{***}	-0.0277^{***}	-0.0432^{***}
	(0.0009)	(0.0069)	(0.0141)
$C^{\text{high}} \odot W^r \cdot \text{event}_t$	-0.0051	0.0074^{***}	0.0213^{***}
	(0.0088)	(0.0015)	(0.0028)
$C^{\text{low}} \odot W^r \cdot \text{event}_t$	0.0141	0.0012	0.0102^{***}
	(0.0087)	(0.0015)	(0.0029)
$\ln(\text{pop}_t)$	0.0249^{***}	0.0258^{***}	0.0244^{***}
	(0.0013)	(0.0013)	(0.0013)
$W^r \cdot \ln(\text{pop})_t$	0.0109^{***}	0.0113^{***}	0.0106^{***}
	(0.0006)	(0.0006)	(0.0006)
$\ln(\text{lights}_{t-1})$	-0.4386^{***}	-0.4367^{***}	-0.4380^{***}
	(0.0011)	(0.0011)	(0.0011)
ρ	0.0672^{***}	0.0672^{***}	0.0672^{***}
	(0.0000)	(0.0000)	(0.0000)
Observations	507,864	502,026	506,037

Note: ***, **, * denote significance at the 1%, 5% and 10% level. All specifications are SDEM and are estimated by Maximum Likelihood. Standard errors in parentheses. Cell and year fixed effects, and first temporal lags of weather events included but not reported. Spatial radius is r=80 km. Yearly disaster intensities reflect time-weighted rolling averages over 12 subsequent monthly observations. $C^i \odot W^r \cdot \text{event}_t$ terms represent corresponding z-scores.

Table A3: Roads Connectivity Thirtiles

Dependent Variable: $\Delta \ln(\text{lights}_t)$			
	wind	**precip.**	**cold**
event_t	−0.0015*	−0.0266***	−0.0350**
	(0.0009)	(0.0069)	(0.0145)
$C^{\text{high}} \odot W^r \cdot \text{event}_t$	−0.0017	0.0057***	0.0113***
	(0.0089)	(0.0015)	(0.0031)
$C^{\text{middle}} \odot W^r \cdot \text{event}_t$	−0.0072	0.0031**	0.0130***
	(0.0090)	(0.0015)	(0.0032)
$C^{\text{low}} \odot W^r \cdot \text{event}_t$	−0.0018	0.0005	0.0086***
	(0.0090)	(0.0015)	(0.0030)
$\ln(\text{pop}_t)$	0.0249***	0.0258***	0.0244***
	(0.0013)	(0.0013)	(0.0013)
$W^r \cdot \ln(\text{pop})_t$	0.0109***	0.0113***	0.0106***
	(0.0006)	(0.0006)	(0.0006)
$\ln(\text{lights}_{t-1})$	−0.4386***	−0.4367***	−0.4380***
	(0.0011)	(0.0011)	(0.0011)
ρ	0.0672***	0.0672***	0.0672***
	(0.0000)	(0.0000)	(0.0000)
Observations	507,864	502,026	506,037

Note: ***, **, * denote significance at the 1%, 5% and 10% level. All specifications are SDEM and are estimated by Maximum Likelihood. Standard errors in parentheses. Cell and year fixed effects, and first temporal lags of weather events included but not reported. Spatial radius is r=80 km. Yearly disaster intensities reflect time-weighted rolling averages over 12 subsequent monthly observations. $C^i \odot W^r \cdot \text{event}_t$ terms represent corresponding z-scores.

Table A4: Wald Chi-Squared Tests: Road Heterogeneity (Two Groups)

H0: Spillover from C^{high} = Spillover from C^{low}			
	wind	**precip.**	**cold**
χ^2	3.4094	12.0510	10.6170
$\Pr(>\chi^2)$	0.06483*	0.0005***	0.0011***

Note: ***, **, * denote significance at the 1%, 5% and 10% level. Tests based on regressions presented in Panel A of Table 3.

Table A5: Wald Chi-Squared Tests: Road Heterogeneity (Three Groups)

	wind	**precip.**	**cold**
H0: Spillover from C^{high} = Spillover from C^{low}			
χ^2	0.0000	7.7980	0.5153
$\Pr(>\chi^2)$	0.9955	0.0052***	0.4728
H0: Spillover from C^{high} = Spillover from C^{medium}			
χ^2	0.1437	1.0921	0.1056
$\Pr(>\chi^2)$	0.7046	0.2960	0.7452
H0: Spillover from C^{medium} = Spillover from C^{low}			
χ^2	0.2350	1.7678	1.3112
$\Pr(>\chi^2)$	0.6278	0.1836	0.2522

Note: ***, **, * denote significance at the 1%, 5% and 10% level. Tests based on regressions presented in Panel B of Table 3.

Table A6: Leaving Out Cells With Less Than Three Neighbors (2 Groups)

Dependent Variable: $\Delta \ln(\text{lights}_t)$			
	wind	**precip.**	**cold**
event_t	-0.0025^{**}	-0.0211^{***}	-0.0738^{***}
	(0.0011)	(0.0080)	(0.0184)
$C^{\text{high}} \odot W^r \cdot \text{event}_t$	-0.0078	0.0060^{***}	0.0241^{***}
	(0.0089)	(0.0015)	(0.0030)
$C^{\text{low}} \odot W^r \cdot \text{event}_t$	0.0099	0.0006	0.0134^{***}
	(0.0088)	(0.0016)	(0.0030)
$\ln(\text{pop}_t)$	0.0198^{***}	0.0213^{***}	0.0195^{***}
	(0.0015)	(0.0015)	(0.0015)
$W^r \cdot \ln(\text{pop})_t$	0.0097^{***}	0.0103^{***}	0.0096^{***}
	(0.0006)	(0.0006)	(0.0006)
$\ln(\text{lights}_{t-1})$	-0.4431^{***}	-0.4415^{***}	-0.4424^{***}
	(0.0011)	(0.0011)	(0.0011)
ρ	0.0672^{***}	0.0672^{***}	0.0672^{***}
	(0.0000)	(0.0000)	(0.0000)
Observations	459,669	453,831	457,947

Note: ***, **, * denote significance at the 1%, 5% and 10% level. All specifications are SDEM and are estimated by Maximum Likelihood. Standard errors in parentheses. Cell and year fixed effects, and first temporal lags of weather events included but not reported. Spatial radius is r=80 km. Yearly disaster intensities reflect time-weighted rolling averages over 12 subsequent monthly observations. $C^i \odot W^r \cdot \text{event}_t$ terms represent corresponding z-scores.

Table A7: Leaving Out Cells With Less Than Three Neighbors (3 Groups)

Dependent Variable: $\Delta \ln(\text{lights}_t)$

	wind	**precip.**	**cold**
event_t	−0.0009	−0.0211***	−0.0583***
	(0.0011)	(0.0080)	(0.0189)
$C^{\text{high}} \odot W^r \cdot \text{event}_t$	−0.0071	0.0045***	0.0121***
	(0.0087)	(0.0015)	(0.0031)
$C^{\text{medium}} \odot W^r \cdot \text{event}_t$	−0.0095	0.0029*	0.0155***
	(0.0088)	(0.0015)	(0.0032)
$C^{\text{low}} \odot W^r \cdot \text{event}_t$	−0.0085	0.0002	0.0110***
	(0.0093)	(0.0016)	(0.0033)
$\ln(\text{pop}_t)$	0.0198***	0.0213***	0.0196***
	(0.0015)	(0.0015)	(0.0015)
$W^r \cdot \ln(\text{pop})_t$	0.0097***	0.0103***	0.0096***
	(0.0006)	(0.0006)	(0.0006)
$\ln(\text{lights}_{t-1})$	−0.4431***	−0.4415***	−0.4424***
	(0.0011)	(0.0011)	(0.0011)
ρ	0.0672***	0.0672***	0.0672***
	(0.0000)	(0.0000)	(0.0000)
Observations	459,669	453,831	457,947

Note: ***, **, * denote significance at the 1%, 5% and 10% level. All specifications are SDEM and are estimated by Maximum Likelihood. Standard errors in parentheses. Cell and year fixed effects, and first temporal lags of weather events included but not reported. Spatial radius is r=80 km. Yearly disaster intensities reflect time-weighted rolling averages over 12 subsequent monthly observations. $C^i \odot W^r \cdot \text{event}_t$ terms represent corresponding z-scores.

Table A8: Leaving Out Cells With Less Than Two Neighbors (2 Groups)

Dependent Variable: $\Delta \ln(\text{lights}_t)$

	wind	**precip.**	**cold**
event_t	-0.0023^{**}	-0.0256^{***}	-0.0753^{***}
	(0.0010)	(0.0075)	(0.0161)
$C^{\text{high}} \odot W^r \cdot \text{event}_t$	-0.0079	0.0070^{***}	0.0246^{***}
	(0.0089)	(0.0015)	(0.0029)
$C^{\text{low}} \odot W^r \cdot \text{event}_t$	0.0116	0.0009	0.0145^{***}
	(0.0088)	(0.0015)	(0.0030)
$\ln(\text{pop}_t)$	0.0248^{***}	0.0257^{***}	0.0242^{***}
	(0.0014)	(0.0014)	(0.0014)
$W^r \cdot \ln(\text{pop})_t$	0.0105^{***}	0.0110^{***}	0.0104^{***}
	(0.0006)	(0.0006)	(0.0006)
$\ln(\text{lights}_{t-1})$	-0.4418^{***}	-0.4401^{***}	-0.4414^{***}
	(0.0011)	(0.0011)	(0.0011)
ρ	0.0672^{***}	0.0672^{***}	0.0672^{***}
	(0.0000)	(0.0000)	(0.0000)
Observations	488,670	482,790	486,990

Note: ***, **, * denote significance at the 1%, 5% and 10% level. All specifications are SDEM and are estimated by Maximum Likelihood. Standard errors in parentheses. Cell and year fixed effects, and first temporal lags of weather events included but not reported. Spatial radius is r=80 km. Yearly disaster intensities reflect time-weighted rolling averages over 12 subsequent monthly observations. $C^i \odot W^r \cdot \text{event}_t$ terms represent corresponding z-scores.

Table A9: Leaving Out Cells With Less Than Two Neighbors (3 Groups)

Dependent Variable: $\Delta \ln(\text{lights}_t)$

	wind	**precip.**	**cold**
event_t	−0.0010	−0.0255***	−0.0638***
	(0.0010)	(0.0075)	(0.0165)
$C^{\text{high}} \odot W^r \cdot \text{event}_t$	−0.0058	0.0059***	0.0134***
	(0.0088)	(0.0015)	(0.0031)
$C^{\text{medium}} \odot W^r \cdot \text{event}_t$	−0.0086	0.0026*	0.0151***
	(0.0089)	(0.0015)	(0.0032)
$C^{\text{low}} \odot W^r \cdot \text{event}_t$	−0.0056	0.0005	0.0125***
	(0.0092)	(0.0015)	(0.0032)
$\ln(\text{pop}_t)$	0.0248***	0.0257***	0.0243***
	(0.0014)	(0.0014)	(0.0014)
$W^r \cdot \ln(\text{pop})_t$	0.0105***	0.0110***	0.0104***
	(0.0006)	(0.0006)	(0.0006)
$\ln(\text{lights}_{t-1})$	−0.4418***	−0.4401***	−0.4413***
	(0.0011)	(0.0011)	(0.0011)
ρ	0.0672***	0.0672***	0.0672***
	(0.0000)	(0.0000)	(0.0000)
Observations	488,670	482,790	486,990

Note: ***, **, * denote significance at the 1%, 5% and 10% level. All specifications are SDEM and are estimated by Maximum Likelihood. Standard errors in parentheses. Cell and year fixed effects, and first temporal lags of weather events included but not reported. Spatial radius is r=80 km. Yearly disaster intensities reflect time-weighted rolling averages over 12 subsequent monthly observations. $C^i \odot W^r \cdot \text{event}_t$ terms represent corresponding z-scores.

Table A10: Consider Only Shortest Connection (2 Groups)

Dependent Variable: $\Delta \ln(\text{lights}_t)$

	wind	**precip.**	**cold**
event_t	-0.0025^{***}	-0.0280^{***}	-0.0410^{***}
	(0.0009)	(0.0069)	(0.0141)
$C^{\text{high}} \odot W^r \cdot \text{event}_t$	-0.0039	0.0082^{***}	0.0221^{***}
	(0.0090)	(0.0015)	(0.0029)
$C^{\text{low}} \odot W^r \cdot \text{event}_t$	0.0128	0.0006	0.0091^{***}
	(0.0088)	(0.0015)	(0.0029)
$\ln(\text{pop}_t)$	0.0249^{***}	0.0258^{***}	0.0244^{***}
	(0.0013)	(0.0013)	(0.0013)
$W^r \cdot \ln(\text{pop})_t$	0.0109^{***}	0.0113^{***}	0.0106^{***}
	(0.0006)	(0.0006)	(0.0006)
$\ln(\text{lights}_{t-1})$	-0.4386^{***}	-0.4367^{***}	-0.4380^{***}
	(0.0011)	(0.0011)	(0.0011)
ρ	0.0672^{***}	0.0672^{***}	0.0672^{***}
	(0.0000)	(0.0000)	(0.0000)
Observations	507,864	502,026	506,037

Note: ***, **, * denote significance at the 1%, 5% and 10% level. All specifications are SDEM and are estimated by Maximum Likelihood. Standard errors in parentheses. Cell and year fixed effects, and first temporal lags of weather events included but not reported. Spatial radius is r=80 km. Yearly disaster intensities reflect time-weighted rolling averages over 12 subsequent monthly observations. $C^i \odot W^r \cdot \text{event}_t$ terms represent corresponding z-scores.

Table A11: Consider Only Shortest Connection (3 Groups)

Dependent Variable: $\Delta \ln(\text{lights}_t)$

	wind	**precip.**	**cold**
event_t	-0.0016^{*}	-0.0275^{***}	-0.0355^{**}
	(0.0009)	(0.0070)	(0.0144)
$C^{\text{high}} \odot W^r \cdot \text{event}_t$	-0.0060	0.0064^{***}	0.0150^{***}
	(0.0104)	(0.0017)	(0.0036)
$C^{\text{medium}} \odot W^r \cdot \text{event}_t$	0.0006	0.0021	0.0082^{**}
	(0.0105)	(0.0017)	(0.0038)
$C^{\text{low}} \odot W^r \cdot \text{event}_t$	-0.0015	0.0006	0.0085^{***}
	(0.0090)	(0.0015)	(0.0030)
$\ln(\text{pop}_t)$	0.0249^{***}	0.0258^{***}	0.0244^{***}
	(0.0013)	(0.0013)	(0.0013)
$W^r \cdot \ln(\text{pop})_t$	0.0109^{***}	0.0113^{***}	0.0106^{***}
	(0.0006)	(0.0006)	(0.0006)
$\ln(\text{lights}_{t-1})$	-0.4386^{***}	-0.4367^{***}	-0.4380^{***}
	(0.0011)	(0.0011)	(0.0011)
ρ	0.0672^{***}	0.0672^{***}	0.0672^{***}
	(0.0000)	(0.0000)	(0.0000)
Observations	507,864	502,026	506,037

Note: ***, **, * denote significance at the 1%, 5% and 10% level. All specifications are SDEM and are estimated by Maximum Likelihood. Standard errors in parentheses. Cell and year fixed effects, and first temporal lags of weather events included but not reported. Spatial radius is r=80 km. Yearly disaster intensities reflect time-weighted rolling averages over 12 subsequent monthly observations. $C^i \odot W^r \cdot \text{event}_t$ terms represent corresponding z-scores.